Article

1,2-Didehydro[10]annulenes: Structures, Aromaticity, and Cyclizations

Armando Navarro-Vzquez, and Peter R. Schreiner

J. Am. Chem. Soc., **2005**, 127 (22), 8150-8159• DOI: 10.1021/ja0507968 • Publication Date (Web): 14 May 2005

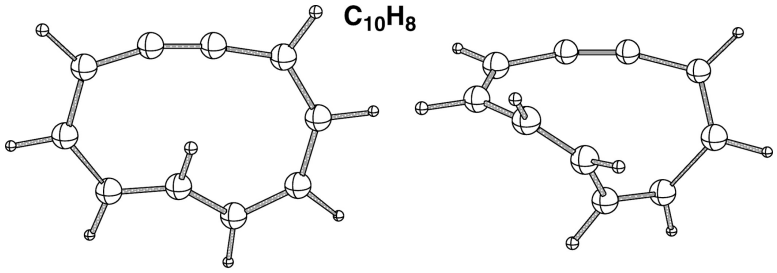

(3*Z*,5*E*,7*Z*,9*Z*) **Aromatic** (3*Z*,5*Z*,7*Z*,9*Z*) **Non-aromatic**

More About This Article

Additional resources and features associated with this article are available within the HTML version:

- Supporting Information
- Links to the 1 articles that cite this article, as of the time of this article download
- Access to high resolution figures
- Links to articles and content related to this article
- Copyright permission to reproduce figures and/or text from this article

View the Full Text HTML

J|A|C|S
ARTICLES
Published on Web 05/14/2005

1,2-Didehydro[10]annulenes: Structures, Aromaticity, and Cyclizations

Armando Navarro-Vázquez[||,‡] and Peter R. Schreiner*[,||,§]

Contribution from the Institute of Organic Chemistry, Justus-Liebig-University, Heinrich-Buff-Ring 58, 35392 Giessen, Germany, Departamento de Química Orgánica y Unidad Asociada al CSIC, Facultade de Química, Universidade de Santiago de Compostela, 15706 Santiago de Compostela, Spain, and Department of Chemistry, Center for Computational Chemistry, The University of Georgia, Athens, Georgia 30602-2556

Received February 7, 2005; E-mail: prs@org.chemie.uni-giessen.de

Abstract: The conformational space of $C_{10}H_8$ 1,2-didehydro[10]annulenes, along with their unimolecular conversion to isonaphthalenes (cyclic allenes), has been studied computationally using DFT (B3LYP), single-reference [CCSD(T)], and multireference (MCQDPT2) post-HF methods. The introduction of the linear alkynyl moiety releases enough angle strain to make a nearly planar "heart" aromatic form the preferred conformer by more than 6 kcal/mol [CCSD(T)] over a localized C_2 "twist" structure, as opposed to the closely related $C_{10}H_{10}$ [10]annulene system. Computations also show that electrocyclic ring-opening of isonaphthalenes to the heart $C_{10}H_8$ annulene takes place through a low barrier of 15 kcal/mol, and this should be considered the working mechanism for the reported isomerizations during dehydro Diels−Alder reactions of phenylacetylenes.

Introduction

The dehydro Diels−Alder (DA) reactions[1] of diaryldiynones **1** and phenylpropiolamides **2** impressively show that sometimes you can teach an old dog new tricks! This is evident from the reports of Echavarren[2] and Saá[3] (Scheme 1) that **1** and **2** give not only the expected "linear" products **3** and **4** but also the rearranged "angular" forms **5** and **6**.

To account for this unexpected change in the carbon skeleton, two different mechanisms were proposed. Both involve two equilibrating cyclic allenes **8** and **10** (Scheme 2), as indicated by isotopic labeling in Saá's work. As possible mechanisms, Echavarren's group proposes equilibration of cyclic allenes **8** and **10** either through the all-*Z* 1,2-didehydro[10]annulene **9** or through carbene **11** from **8** and then ring contraction to **10**. Saá and co-workers, on the basis of B3LYP/6-31G* computations, proposed a mechanism involving also a [10]annulene, but in its trans form **12**. Thermal equilibration of **12** with its isomer **13** would eventually also give **10**. In both mechanisms, the final products would be aromatic after isomerization of the intermediate cyclic allenes.[4] This aromatization step has recently been carefully studied, both experimental and computationally.[5]

The structures of $C_{10}H_{10}$ [10]annulene have been the object of detailed theoretical studies[6] ranging from force field MM3[6a] to CCSD(T)[6d,e] computations, which were necessary in order to appropriately describe the energy difference between the isomers. A "twist" localized form is favored over "naphthalene-like" and "heart" forms. On the other side, DFT and MP2 computations fail miserably with a strong tendency to overestimate the stability of aromatic forms. Due to the highly delocalized nature of annulenes, the amount of the nonlocal HF component in the exchange functional seems to be crucial in the DFT description of these systems.[7] Thus, BHandhLYP functional, with 50% HF exchange, gives relative energies closer to CCSD(T) results than those obtained with B3LYP or the pure functional BP86.[6f] However, B3LYP geometries are closer to those obtained from CCSD(T) optimizations, and single-point CCSD(T)//B3LYP computations on [10]annulenes[6c] as well as aza[10]annulenes[8] gave results close to those resulting from much more time-consuming CCSD(T) geometry optimizations.[6d] Hence, coupled-cluster energies on B3LYP-optimized geometries seemed to us the appropriate level of theory to investigate the $C_{10}H_8$ annulene potential energy surface.

[||] Justus-Liebig-University.
[‡] Universidade de Santiago de Compostela.
[§] The University of Georgia.

(1) Michael, A.; Bucher, J. E. *Chem. Ber*. **1895**, *28*, 2511−2512.
(2) Atienza, C.; Mateo, C.; de Frutos, O.; Echavarren, A. M. *Org. Lett*. **2001**, *3*, 153−155.
(3) Rodríguez, D.; Navarro-Vázquez, A.; Castedo, L.; Domínguez, D.; Saá, C. *J. Am. Chem. Soc*. **2001**, *123*, 9178−9179.
(4) Hopf, H.; Musso, H. *Angew. Chem., Int. Ed. Engl*. **1969**, *8*, 680−682.
(5) (a) Fernández-Zertuche, M.; Hernández-Lamoneda, R.; Ramírez-Solís, A. *J. Org. Chem*. **2000**, *65*, 5207−5211. (b) Prall, M.; Krüger, A.; Schreiner, P. R.; Hopf, H. *Chem. Eur. J*. **2001**, *7*, 4386−4394. (c) Ananikov, V. P. *J. Phys. Org. Chem*. **2001**, *14*, 109−121. (d) Rodríguez, D.; Navarro-Vázquez, A.; Castedo, L.; Domínguez, D.; Saá, C. *J. Org. Chem*. **2003**, *68*, 1938−1946.
(6) (a) Xie, Y.; Schaefer, H. F., III; Liang, G.; Bowen, J. P. *J. Am. Chem. Soc*. **1994**, *116*, 1442−1449. (b) Sulzbach, H. M.; Schleyer, P. v. R.; Jiao, H.; Xie, Y.; Schaefer, H. F., III. *J. Am. Chem. Soc*. **1995**, *117*, 1369−1373. (c) Sulzbach, H. M.; Schaefer, H. F., III; Klopper, W.; Lüthi, H. P. *J. Am. Chem. Soc*. **1996**, *118*, 3519−3520. (d) King, R. A.; Crawford, T. D.; Stanton, J. F.; Schaefer, H. F., III. *J. Am. Chem. Soc*. **1999**, *121*, 10788−10793. (e) Price, D. R.; Stanton, J. F. *Org. Lett*. **2002**, *4*, 2809−2811. (f) Orlova, G.; Goddard, J. D. *Mol. Phys*. **2002**, *100*, 483−497 (g) Sancho-García, J. C. *J. Chem. Phys. A* **2005**, *109*, 3470−4375.
(7) Woodcock, H. L.; Schaefer, H. F., III; Schreiner, P. R. *J. Phys. Chem. A* **2002**, *106*, 11923−11931.
(8) Bettinger, H. F.; Sulzbach, H. M.; Schleyer, P. v. R.; Schaefer, H. F., III. *J. Org. Chem*. **1999**, *64*, 3278−3280.

10.1021/ja0507968 CCC: $30.25

Scheme 1. Rearrangements of Phenylacetylene Derivatives via Dehydro Diels−Alder Reactions

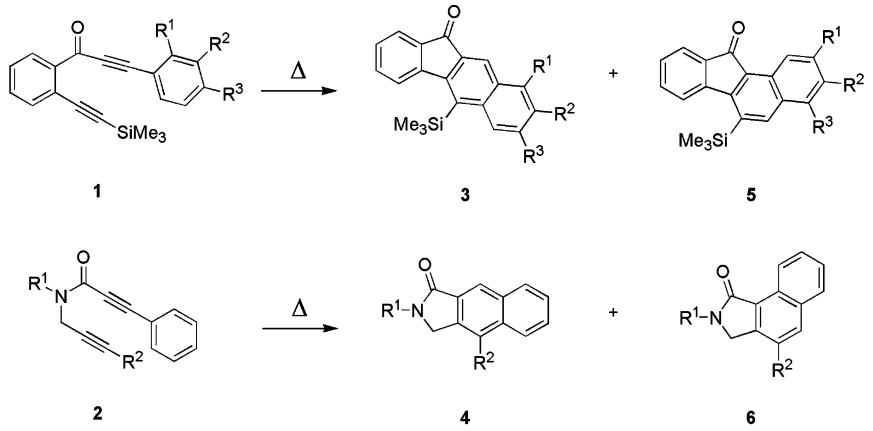

Scheme 2. Echavarren (left) and Saá (right) Proposed Mechanisms for the Rearrangement of Phenyl−Acetylene Alkyne Derivatives through Dehydro Diels−Alder Reactions (The Dashed Line Implies Alternative Positions of the Double Bond)

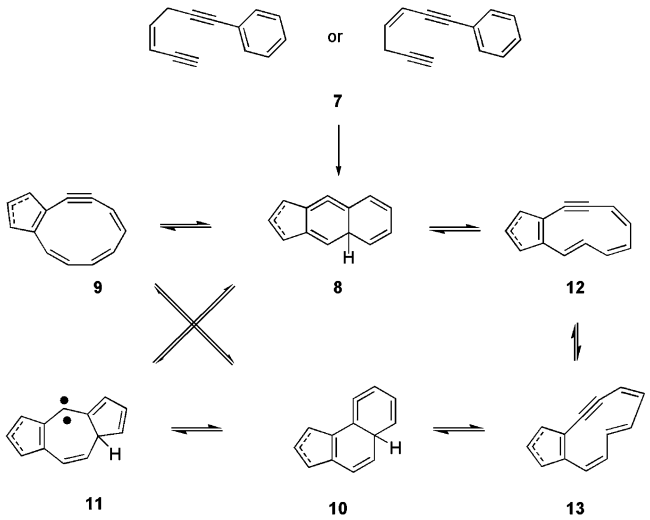

Thus, due to the novelty of this rearrangement, which involved several new high-energy species not studied until now, we decided to start a full quantum mechanical characterization of the potential surface related to these reactions. This study allows us to discern between the different mechanistic possibilities and provides insights into the nature of didehydro[10]-annulenes that are virtually unknown species.[9]

Computational Methodology

A computational problem that arises in this work is that both closed-shell and open-shell singlet species are involved. Although proper treatment of biradicals may require the use of multiconfigurational approaches, it is known that density functional theory (DFT)[10] methods can handle both by using a single Kohn−Sham MO determinant.[11] However, for many biradicals, it is possible to obtain a lower energy using an unrestricted determinant allowing α and β densities to occupy different spatial regions.[12] This different spatial distribution is manifested by nonzero $\langle S^2 \rangle$ spin-squared expectation values directly computed on the unrestricted determinant as in a Hartree−Fock system. In this work, an unrestricted formalism was used in the DFT computations for all species with biradical character. The HOMO and LUMO orbitals were mixed in the initial guess, allowing the MO determinant to break spin symmetry if necessary.[13] All structures were optimized using the hybrid B3LYP functional.[14] The 6-31G*[15] basis set was used for all geometry optimizations with analytic gradients. Analytic calculation of the Hessian matrix and further diagonalization was used to verify the nature of the stationary points located in DFT optimizations. ZPVE corrections were computed at the B3LYP/6-31G* level and were scaled with a factor of 0.9804.[16] In particular cases, geometries and harmonic vibrational frequencies were also computed at the MP2[17] and QCISD[18] levels (in this case, Hessian was computed numerically), using the Dunning correlation consistent basis set cc-pVDZ[19] in its spherical harmonics expression (i.e., 5d). For all computed transition structures, the eigenvector associated with the imaginary frequency was visualized to verify that the saddle point connects the expected reactant and products.[20]

Single-point B3LYP energy computations were performed on the optimized DFT structures using a larger 6-311G** basis set.[15] Bond orders were determined by the Wiberg method[21] using the B3LYP/6-311G* densities, in the basis of NAO orbitals.[22]

The DFT results were checked against post-HF methods. Multiconfigurational CASSCF[23] single-point energy computations were performed on the B3LYP/6-31G* structures involved in the cyclization and aromatization steps. The chosen (12,12) active space in cyclizations consisted of the orbitals involved in bonding changes, that is, all valence π and π^* orbitals and the new σ and σ^* orbitals formed during the

(9) Only a relatively low-level MP2/6-31G*//HF/6-31G* study exists for 1, 2-didehydro[10]annulenes: Yavari, I.; Norouzi-Arasi, H. *J. Mol. Struct. (THEOCHEM)* **2002**, *593*, 199−207.
(10) Parr, R.; Yang, W. *Density Functional Theory of Atoms and Molecules*; Oxford University Press: New York, 1989.
(11) Kohn, W.; Sham, L. J. *Phys. Rev. A.* **1965**, 1133−1138.
(12) (a) Bauernschmitt, R.; Ahlrichs, R. *J. Chem. Phys.* **1996**, *104*, 9047−9052. (b) Crawford, T. D.; Kraka, E.; Stanton, J. F.; Cremer, D. *J. Chem. Phys.* **2001**, *114*, 10638−10650. (c) Gräfenstein, J.; Kraka, E.; Filatov, M.; Cremer, D. *Int. J. Mol. Sci*. **2002**, *3*, 360−394. (d) Cremer, D.; Filatov, M.; Polo, V.; Kraka, E.; Shaik, S. *Int. J. Mol. Sci.* **2002**, *3*, 604−638. (e) Polo, V.; Kraka, E.; Cremer, D. *Theor. Chem. Acc*. **2002**, *107*, 291−303.
(13) For applications, see: (a) Cramer, C. J. *J. Am. Chem. Soc.* **1998**, *120*, 6261−6269. (b) Schreiner, P. R.; Navarro-Vázquez, A.; Prall, M. *Acc. Chem. Res*. **2005**, *38*, 29−37.
(14) (a) Becke, A. D. *J. Chem. Phys.* **1993**, *98*, 5648−5652. (b) Lee, C.; Yang, W.; Parr, R. G. *Phys. Rev. B.* **1988**, *37*, 785−789.
(15) Hehre, W.; Radom, L.; Schleyer, P. v. R.; Pople, J. A. *Ab Initio Molecular Orbital Theory*; Wiley: New York, 1986.
(16) Wong, M. W. *Chem. Phys. Lett*. **1996**, *256*, 391−399.
(17) (a) Frisch, M. J.; Head-Gordon, M.; Pople, J. A. *Chem. Phys. Lett*. **1990**, *166*, 281−289. (b) Head-Gordon, M.; Head-Gordon, T. *Chem. Phys. Lett*. **1994**, *220*, 122−128.
(18) Pople, J. A.; Head-Gordon, M.; Raghavachari, K. *J. Chem. Phys*. **1987**, *87*, 5968−5975.
(19) (a) Dunning, T. H. Jr. *J. Chem. Phys*. **1989**, *90*, 1007−1023. (b) Davidson, E. R. *Chem. Phys. Lett*. **1996**, *260*, 514−518.
(20) To animate normal modes and display molecular orbitals, the MOLDEN program was used: Schaftenaar, G. *MOLDEN (A Pre- and Postprocessing Program of Molecular and Electronic Structure);* CAOS/CAMM Center: University of Nijmegen: Nijmegen, The Netherlands (http://www.cmbi.ru.nl/molden/molden.html).
(21) Wiberg, K. B. *Tetrahedron* **1968**, *24*, 1083−1096.
(22) Reed, A. E.; Curtiss, L. A.; Weinhold, F. *Chem. Rev*. **1988**, *88*, 899−926.
(23) Schmidt, M. W.; Gordon, M. S. *Annu. Rev. Phys. Chem*. **1998**, *49*, 233−266.

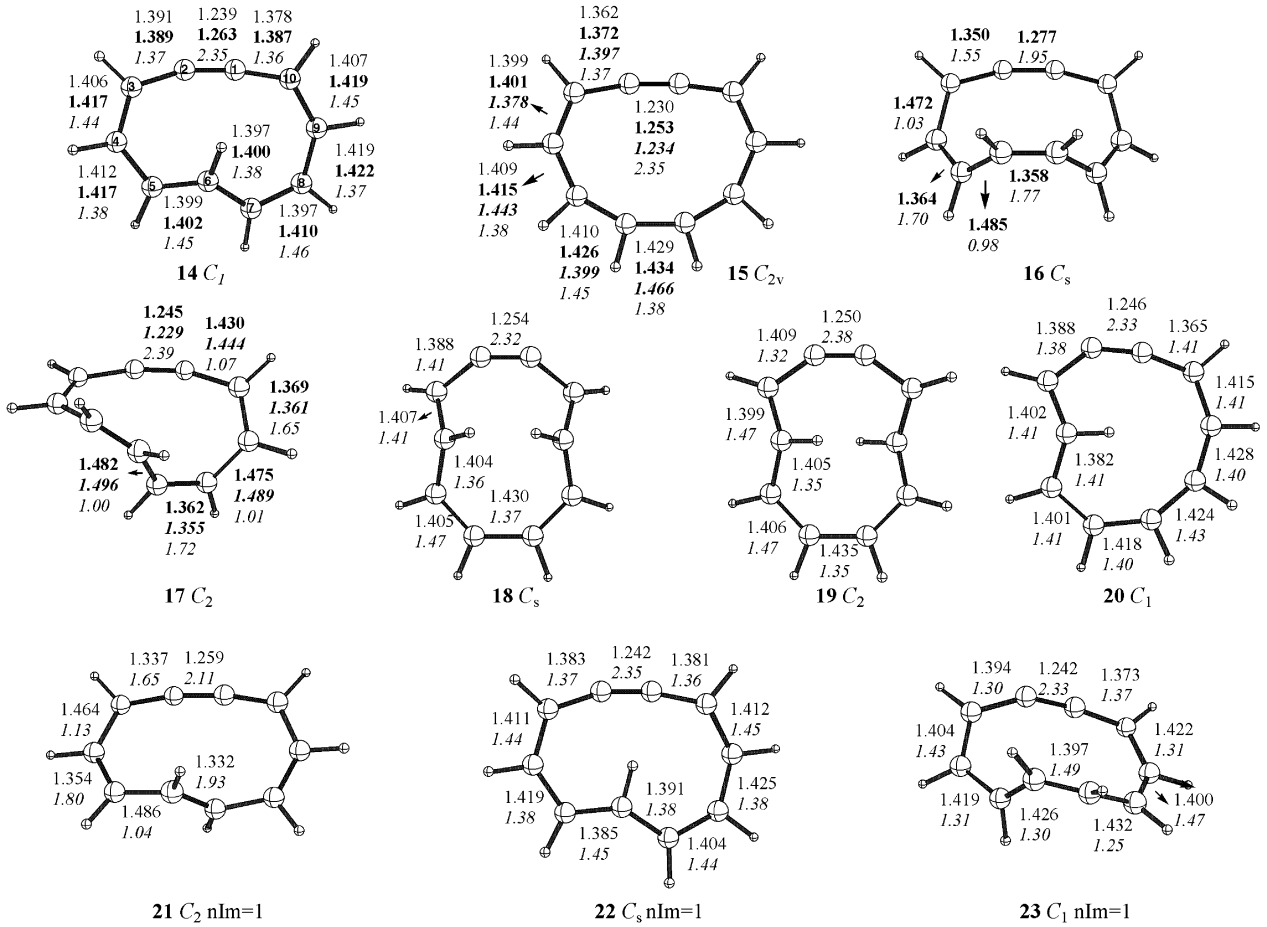

Figure 1. 1,2-Didehydro[10]annulene conformers (**14**−**20**) and transition structures (**21**−**23**) for conformational interconversion. Bond lengths: B3LYP/6-31G*, bold MP2/cc-pVDZ, bold italics QCISD/cc-pVDZ. In italics, Wiberg bond indexes derived from B3LYP/6-311G** densities (with the exception of **16** and **17**: MP2/cc-pVDZ densities).

Table 1. Relative Energies (ΔH_0, kcal/mol) for $C_{10}H_8$ Annulene Isomers and Interconversion Transition States

	Species									
level	**14**	**15**	**16**	**17**	**18**	**19**	**20**	**21**	**22**	**23**
B3LYP/6-311G**[a]	0.0	12.2			47.9	51.6	36.7	17.4	4.3	40.4
MP2/cc-pVDZ[b]	0.0	16.9	31.1	16.1						
QCISD/cc-pVDZ[c]	0.0	16.8		4.5						
MCQDPT2/cc-pVDZ[a]	0.0	18.0			46.1	45.7	34.9	16.3	4.8	36.5
CCSD(T)/cc-pVDZ[a]	0.0	17.0			45.6	46.6	36.6	13.5	4.7	46.3[d]
CCSD(T)/cc-pVDZ[b]	0.0	16.6	17.7	6.8						

[a] B3LYP/6-31G* geometries. ZPVE corrections taken at B3LYP/6-31G* and scaled by 0.9804. [b] MP2/cc-pVDZ geometries. ZPVE corrections taken at the MP2/cc-pVDZ level unscaled. [c] QCISD/cc-pVDZ geometries. ZPVE corrections taken at the QCISD/cc-pVDZ level unscaled. [d] Value of 46.4 kcal/mol at BD(T)/cc-pVDZ and 45.3 kcal/mol at UCCSD(T)/cc-pVDZ.

cyclizations. For aromatization reactions, the C−C σ and σ^* orbitals were substituted by the corresponding C−H σ and σ^* orbitals involved in those steps, except for the computation of the overall enthalpies, $\Delta H_{0\ 28->35}$ and $\Delta H_{0\ 29->39}$, for which a (10,10) space involving only the π and π^* orbitals was used. However, to obtain meaningful reaction energies, inclusion of dynamic correlation is necessary. This was accomplished at the MP2 level of theory using the multireference perturbation method of Nakano (MCQDPT2),[24] for which the calculated CAS wave functions were used as the reference. This has been show to perform nearly *en par*[25] with the most popular CASPT2 method.[26] Further single-point single-reference coupled-cluster[27] computations on B3LYP/6-31G* geometries were performed at the full coupled-cluster singles and doubles level (CCSD[28]). The effect of triple excitations was computed in a noniterative perturbative manner [CCSD(T)[29]] using the RHF wave function as the reference. For some structures of a high biradical nature, Brueckner doubles BD(T)[30] and unrestricted UCCSD(T) computations were also performed. All post-HF computations, including MCQDPT2, were performed using the frozen-core approximation in which the core orbitals are excluded from the correlation computations and used the cc-pVDZ basis, again, in its spherical harmonics expression.

NMR chemical shifts and NICS[31] were computed at the B3LYP/6-311G**//B3LYP/6-31G* level using the GIAO[32] method, whereas magnetic susceptibilities were computed at B3LYP/6-311G**//B3LYP/6-31G* and B3LYP/6-311G**//MP2/cc-pVDZ using the CSGT[33] method.

(24) (a) Nakano, H. *J. Chem. Phys*. **1993**, *99*, 7983−7992. (b) Nakano, H. *Chem. Phys. Lett*. **1993**, *207*, 372−378.
(25) Sølling, T. I.; Smith, D. M.; Radom, L.; Freitag, M. A.; Gordon, M. S. *J. Chem. Phys*. **2001**, *115*, 8758−8772.
(26) Andersson, K.; Malmqvist, P.-Å.; Roos, B. O. *J. Phys. Chem*. **1992**, *96*, 1218−1226.
(27) Bartlett, R. J. Coupled-Cluster Theory: An Overview of Recent Developments. In *Modern Electronic Structure Theory*; Yarkony, D. R., Ed.; World Scientific: River Edge, NJ, 1995; pp 1047−1131.
(28) (a) Cizek, J. *Adv. Chem. Phys*. **1969**, *14*, 35−89. (b) Purvis, G. D.; Bartlett, R. J. *J. Chem. Phys*. **1982**, *76*, 1910−1918. (c) Scuseria, G. E.; Janssen, C. L.; Schaefer, H. F., III. *J. Chem. Phys*. **1988**, *89*, 7382−7387. (d) Scuseria, G. E.; Schaefer, H. F., III. *J. Chem. Phys*. **1989**, *90*, 3700−3703.
(29) Raghavachari, K.; Trucks, G. W.; Pople, J. A.; Head-Gordon, M. *Chem. Phys. Lett*. **1989**, *157*, 479−483.
(30) Handy, N. C.; Pople, J. A.; Head-Gordon, M.; Raghavachari, K.; Trucks, G. W. *Chem. Phys. Lett*. **1989**, *164*, 185−192.

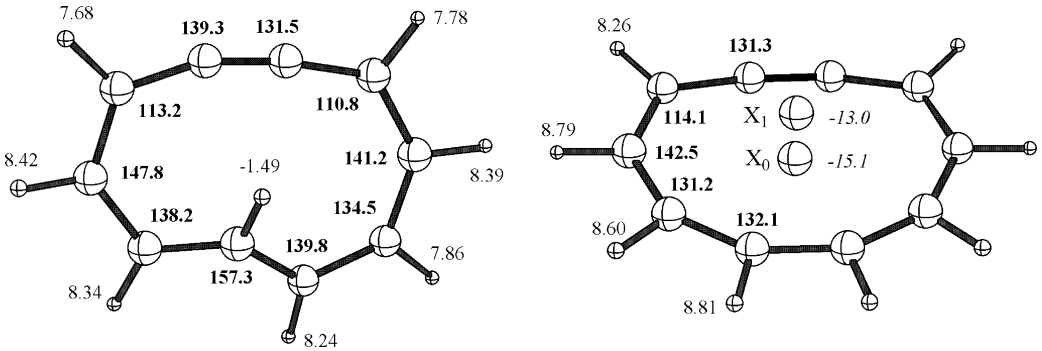

Figure 2. ^{1}H (normal) and ^{13}C δ (ppm) chemical shifts (bold) for **14** and **15** and NICS (italic) for points above 0.0 (X_0) and 1.0 Å (X_1) over the center of the ring.

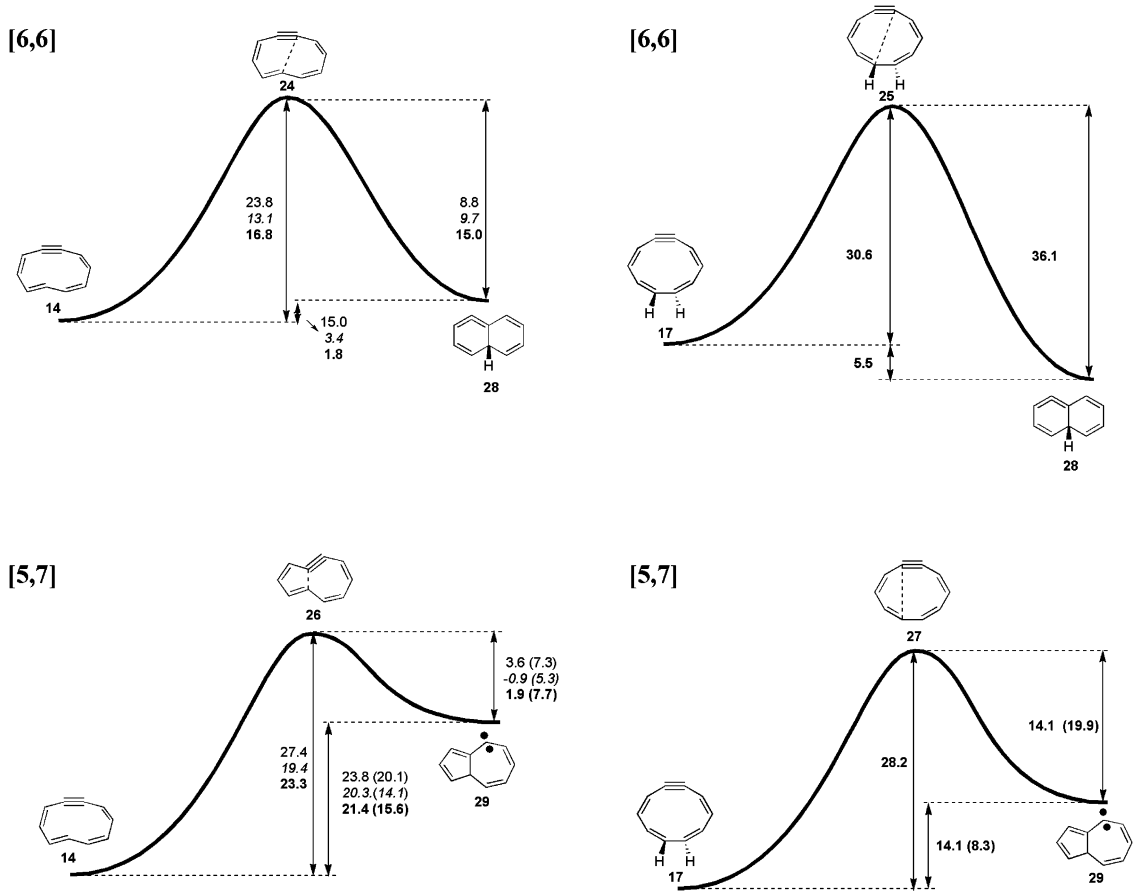

Figure 3. Enthalpy profiles (ΔH_0 in kcal/mol) for the cyclizations of 1,2-didehydro[10]annulenes. Normal B3LYP/6-311G**, italics MCQDPT2/cc-pVDZ, bold CCSD(T)/cc-pVDZ. Values for cyclization to ^{3}A-**29** are in parentheses.

DFT and post-HF computations were performed with the Gaussian 98 program package.[34] All multiconfigurational computations were performed with the GAMESS-US[35] program.

Results and Discussion

1. Structural Properties of the 1,2-Didehydro[10]annulenes. The Conformational Space of 1,2-Didehydro[10]annulenes. 1,2-Didehydro[10]annulene spans a conformational space similar to that of its "all-ene" partner, although it is somewhat more restricted due to the $C^{10}-C^{1}-C^{2}-C^{3}$ linear disposition imposed by the triple bond. The lowest energy form for 1,2-didehydro-[1,2]annulene is the (3*Z*,5*E*,7*Z*,9*Z*) C_1 form **14** (termed "heart" for [10]annulene) that places the H^6 proton near the center of the ring. As could be expected for a nearly planar 10-electron system, the molecule exhibits bond equalization, one of the signs of aromaticity, as evident from the bond distances and Wiberg bond indexes (Figure 1). However, as the $C_{10}H_{10}$ parent, the system is slightly twisted ($\angle C^4-C^5-C^6-H^6 = 24°$) in order to maximize overlap while minimizing the alkyne-H^6 steric repulsion. Hence, replacement of one of the double bonds for an alkyne moiety provides enough angle strain release to allow a quasi-planar aromatic form to be the most stable minimum.

(31) Schleyer, P. v. R.; Maerker, C.; Dransfeld, A.; Jiao, H.; Hommes, N. J. R. v. E. *J. Am. Chem. Soc.* **1996**, *118*, 6317−6318.
(32) Wolinski, K.; Hinton, J. F.; Pulay, P. *J. Am. Chem. Soc.* **1990**, *112*, 8251−8260.
(33) Keith, T. A.; Bader, R. F. W. *Chem. Phys. Lett.* **1993**, *210*, 223−231.
(34) Frisch, M. et al. *Gaussian 98*, revision A.7; Gaussian, Inc.: Pittsburgh, PA, 1998.
(35) Schmidt, M. W. et al. *J. Comput. Chem.* **1993**, *14*, 1347−1363.

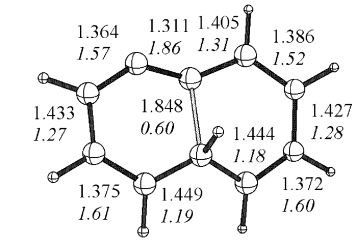

24 C_1

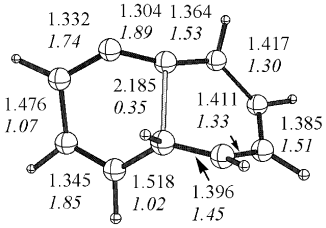

25 C_1

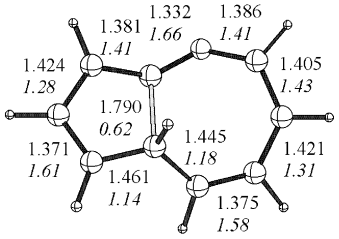

26 C_1

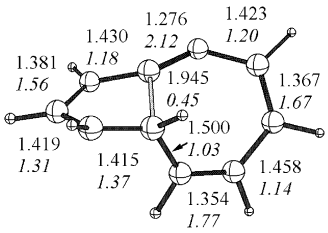

27 C_1

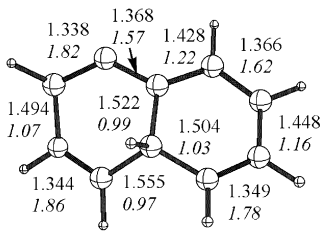

28 C_1

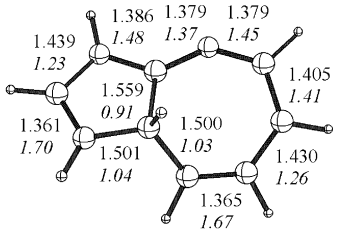

^{1}**A-29** C_1

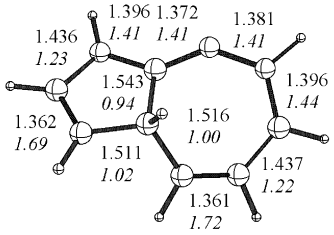

^{3}**A-29** C_1

Figure 4. Transition structures and products for the 1,2-didehydro[10]annulene cyclizations. B3LYP/6-31G* bond lengths in normal style. Wiberg bond indexes on B3LYP/6-311G** densities in italics.

The (3*Z*,5*Z*,7*Z*,9*Z*) configuration can adopt a planar C_{2v} geometry **15**. As found for **14**, this aromatic structure is nearly bond-equalized. However, due to the ring strain, this form is energetically disfavored by 12.2 kcal/mol (B3LYP) relative to **14**. Single-point energies computed at MCQDPT2 and CCSD(T) levels increase this energy gap to 18.0 and 17.0 kcal/mol, respectively (Table 1). To verify that the planarity of **15** was not an artifact due to overestimation of aromaticity in DFT computations, we also optimized and computed frequencies at the MP2/cc-pVDZ and QCISD/cc-pVDZ levels. Whereas **15** is also a minimum at the MP2/cc-pVDZ level, at the QCISD/cc-pVDZ level, this structure is a first-order saddle point (NIMAG $= 51.8i$ cm^{-1} for the A_2 mode). The low absolute value of the frequencies (below 100 cm^{-1}) for B_1 and A_2 modes, associated with out of plane distortions, indicates the floppy character of the molecule in this configuration (vide infra).

We located two other conformers of the (3*Z*,5*Z*,7*Z*,9*Z*) configuration, namely, the C_s (**16**) and the C_2 form (**17**). The C_s form, termed "boat" in the $C_{10}H_{10}$ analogue, does not exist on the B3LYP/6-31G* surface as a minimum and is rather an inflection point for interconversion of **14** and **15** (see below); all attempts to optimize it at B3LYP led to the C_{2v} form **15**. However, when optimizing at MP2/cc-pVDZ, **16** resulted in a true minimum structure, 13.2 kcal/mol above **15**; this difference

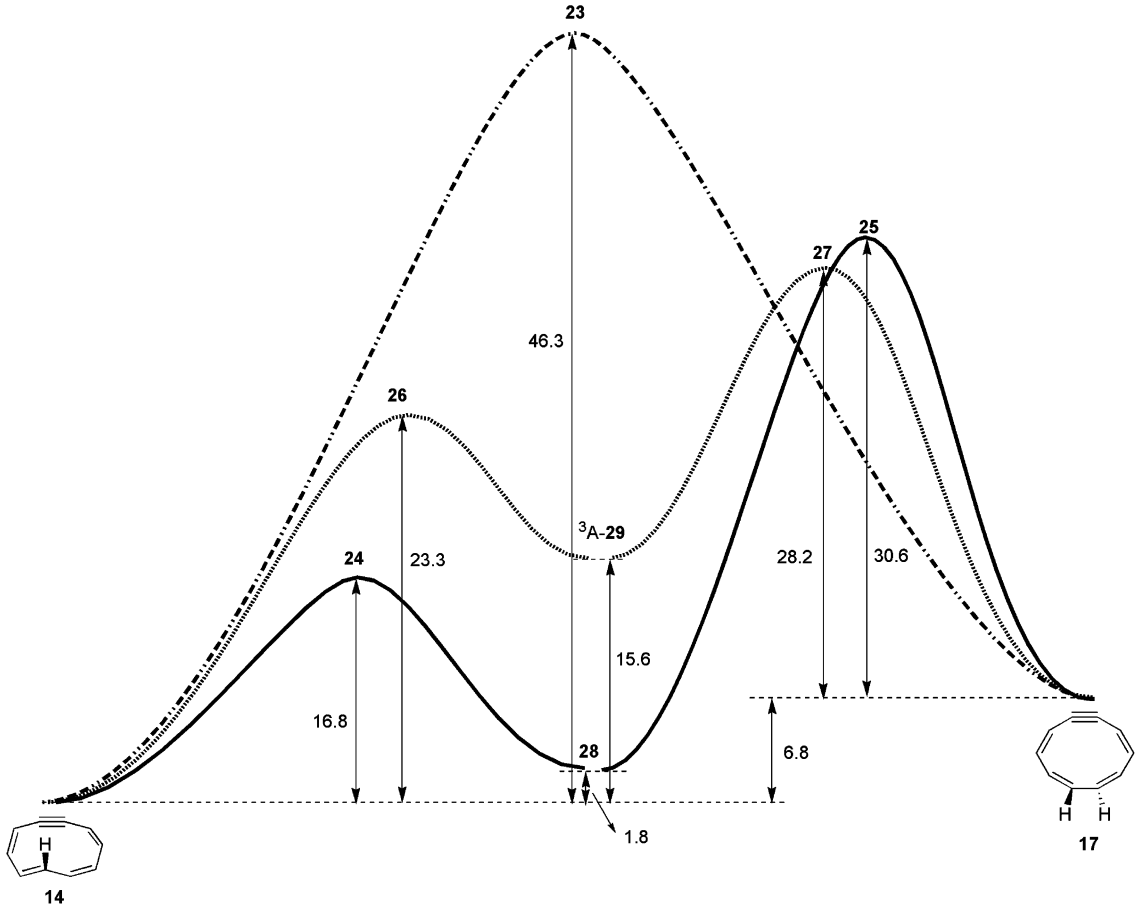

Figure 5. Interconversion pathways between (3*Z*,5*E*,7*Z*,9*Z*) heart **14** and (3*Z*,5*Z*,7*Z*,9*Z*) twist **17** species. Enthalpies (ΔH_0, kcal/mol) taken from the CCSD(T)//B3LYP/6-31G* and CCSD(T)/cc-pVDZ//MP2/cc-pVDZ computations.

Table 2. Computed Magnetic Susceptibilities (ppm cgs) and Magnetic Susceptibility Exaltations

Level	B3LYP/6-311G**//B3LYP/6-31G*		B3LYP/6-311G**//MP2/cc-pVDZ	
species	χ_M	Λ	χ_M	Λ
14	−105.3	−41.0	−105.3	−41.0
15	−115.8	−51.5	−116.1	−51.8
16			−61.4	−2.9
17			−59.6	−4.7
18	−103.3	−39.0		
19	−93.3	−29.0		
20	−111.2	−46.9		
23	−8.8	+55.5		

is reduced to 1.1 kcal/mol at CCSD(T)/cc-pVDZ//MP2/cc-pVDZ. This small energy difference and the low absolute values of the frequencies related to the normal mode associated with the C^5-C^6 out of plane movement show the highly floppy character of the all-*Z* configuration. The C_2 form, resembling the C_2 twist absolute minimum (**17**) on the $C_{10}H_{10}$ surface, was also recently reported[9] as the absolute minimum for 1, 2-didehydro[10]annulene. **17** does not exist as a stationary point on the B3LYP surface but is also a minimum at MP2/cc-pVDZ that is 16.1 kcal/mol above the heart form **14**, that is, 1.1 kcal/mol below the C_{2v} aromatic form. The CCSD(T) computations increase the preference for this twist form but place it only 6.8 kcal/mol above **14**. According to bond lengths, twist **17** presents a localized structure, but as a consequence of twisting, this species presents a phase change in its π system and can be classified as a 10-electron antiaromatic Möbius[36] system, which inhibits electronic delocalization. As a consequence, in its (3*Z*,5*E*,7*Z*,9*Z*) configuration, didehydro[10]annulene adopts a nearly planar aromatic form (**14**), whereas the all-*Z* configuration prefers a localized twist form (**17**) according to our CCSD(T) predictions.

Other high-energy conformers found were the C_s **18** and C_2 **19** conformers with the (3*E*,5*Z*,7*Z*,9*E*) configuration; these two forms are energetically very close. Multireference computations favor the C_2 over the C_s form, whereas both B3LYP and CCSD(T) predict the C_s form to be more stable than C_2 **19**. The (3*E*,5*Z*,7*Z*,9*Z*) configuration displays a more favorable C_1 structure **20** that is placed 36.6 kcal/mol [CCSD(T)] above **14**. Although all of these structures possess aromatic character, the considerable strain caused by the 3*E* and 9*E* double-bond configurations makes them energetically unfavorable.

Interconversion between Low-Energy Conformers. Degenerate interchange of the annulene **14**, one of the key steps in Saá's rearrangement mechanism (Scheme 2), can take place easily through simultaneous rotation of the C^5-C^6 and C^7-C^8 bonds; the transition state for this process (**21**, Figure 1) is a localized structure with C_2 symmetry. At B3LYP, this process is associated with a barrier of 17.4 kcal/mol, while MCQDPT2 and CCSD(T) furnish lower values of 16.3 and 13.5 kcal/mol, respectively (Table 1).

Moreover, **14** can be interconverted with its enantiomer through the C_s planar form **22** with a barrier of only 4.3−4.8 kcal/mol. This means that in the Saá mechanism each en-

(36) Zimmerman, H. E. *Acc. Chem. Res.* **1971**, *4*, 272−280.

Scheme 3. Structures along the Ring Contraction Mechanism

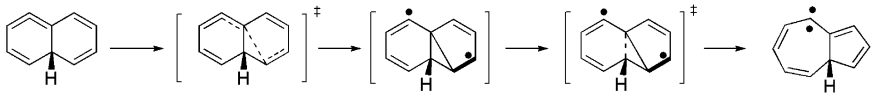

28 **30** **31** **32** **29**

Table 3. Relative Energies ΔH_0 (kcal/mol) for Species Involved in Echavarren's Mechanism

	Species				
level	**28**	**30**	^{3}A-**30**	^{1}A-**31**	^{1}A-**32**
B3LYP/6-311G**	0.0	38.7	39.6	28.0	27.7

Table 4. Relative Energies ΔH_0 (kcal/mol) for the Isonaphthalene **28** Isomerization

	Species		
level	**28**	**33**	**35**
B3LYP/6-311G**[a]	0.0	17.2	−98.7
MCQDPT2/cc-pVDZ[a]	0.0	29.1	−90.4
CCSD(T)/cc-pVDZ[a]	0.0	23.9	−91.7

[a] Single point on B3LYP/6-31G* geometries.

antiomer of the cyclic allene **8** would produce the two possible enantiomers of **10**. Ring inversion of twist **17** takes place through **15**, as indicated by normal-mode analysis on the QCISD frequency computations; the associated barrier is 9.7 kcal/mol at CCSD(T)/cc-pVDZ//MP2/cc-pVDZ.

Notably, formal double-bond isomerization from the (3*Z*,5*E*,7*Z*,9*Z*) configuration in **14** to the (3*Z*,5*E*,7*Z*,9*Z*) in **17** takes place through the C_1 structure **23**, which can be considered as a delocalized "phantom" transition structure. An antiaromatic system arises as a consequence of the Möbius topology of this 10 π-electron system, as manifested by bond equalization and a largely positive magnetic susceptibility exaltation (vide infra). Hence, **23** is biradicaloid, as evident from the instability of the restricted B3LYP determinant; the lowest energy is obtained when a broken-spin-symmetry ansatz ($\langle S^2 \rangle = 1.00$ at B3LYP/6-311G**) is employed. In the CASSCF expansion, single excitations only contribute 5%, while the principal contribution to the multireference expansion comes from the double excitation from HOMO to LUMO (30%). Thus, we can expect that closed-shell coupled-cluster methods, which can be severely affected by large single excitation amplitudes, deal reasonably well with this problem. Both closed-shell methodologies CCSD(T), BD(T) and unrestricted UCCSD(T) computations furnish high activation enthalpies around 45−46 kcal/mol. DFT computations (40.4 kcal/mol) and especially MCQDPT2 (36.5 kcal/mol) give lower values. We will see below that this isomerization can take place more easily through an alternative cyclization mechanism (Figure 5).

NMR Computations. The aromatic nature of 1,2-didehydro-[10]annulene in its forms **14** and **15** should be apparent from their NMR properties.[6] Thus, GIAO-B3LYP/6-311G** chemical shift computations of **14** gave very characteristic values for an aromatic system ($\delta_{H6} = -1.5$ ppm for the inner proton and $\delta = 7.7-8.4$ ppm for the outside protons; Figure 2). The principal difference in the ^{13}C NMR spectra of both compounds is the deshielding of the inner carbon C^6 of 157.3 ppm in **14**. The all-*Z* form **15** has NICS values of −15.1 and −13.0 ppm for points at 0 and 1.0 Å above the center of the ring, which clearly indicates strongly aromatic character.

Another magnetic criterion of aromaticity that has extensively been used is the exaltation of the magnetic susceptibility, Λ, which is defined as the difference between the found (computed) susceptibility, χ_M, for a given compound and that estimated (χ_M') for a cyclopolyene of the same structure.[37]

$$\Lambda = \chi_M - \chi_M' \qquad (1)$$

For $C_{10}H_8$ annulene, we estimate a χ_M' of −64.3 ppm cgs, according to the Haberditzl system.[37,38] Whereas both **14** and **15** present strong exaltations (−41.0 and −51.5 ppm cgs, respectively), these are negligible for the localized boat and twist structures **16** and **17** (Table 2). On the other hand, structure **23** displays a strong positive enhancement (+55.5 ppm cgs), confirming its antiaromatic nature.

IR Spectra. With the aim of providing accurate IR data for future matrix isolation experiments, we computed harmonic frequencies for the heart **14** and twist **17** isomers at QCISD/cc-pVDZ. The most prominent difference between these species is the presence of intense bands at 1028 and 1051 cm^{-1} associated with the wagging of the inner proton H^6 in the spectrum of **14** (see the Supporting Information).

2. Cyclization Reactions of 1,2-Didehydro[10]annulenes. The [6,6]-Cyclizations. Cyclization of heart annulene **14** to cyclic allene **28**[39] takes place through transition structure **24**. As shown in Figure 3, the B3LYP computations overestimate the **14** → **28** energy separation with respect to both CCSD(T), as well as MCQPT2 methods, and the predicted B3LYP energy barrier is also larger. Note that both the forward (16.8 kcal/mol) and reverse barriers (15.0 kcal/mol) are sufficiently large to allow the distinction of the annulene and cyclic allene intermediates in future matrix isolation experiments.

The C_2 twist form **17** can cyclize to the allene **28** through the transition structure **25**. Note that this structure requires much more geometric and energetic deformation than in the cyclizations discussed so far. The transition structure is located in a region where the C^1−C^6 bond has formed much less (the C^1−C^6 distances are 1.848 and 2.185 Å in **24** and **25**, respectively). Since **17** is not a stationary point at the B3LYP/6-31G* level, we have estimated the CCSD(T) barrier and reaction enthalpy by summing up the energy difference between the C_{2v} **15** and **17** conformers at CCSD(T)//MP2 (9.7 kcal/mol) to the CCSD(T)//B3LYP enthalpies, which gives for **17** → **28** a reaction enthalpy of $\Delta H_0 = -5.5$ kcal/mol. The forward and reverse barriers $\Delta H_0^{\ddagger}$ are 30.6 and 36.1 kcal/mol, respectively (Figure 3). As the former value is below the estimated reverse barrier for the **17** → **14** interconversion through transition state **23** (ca. 40 kcal/mol), this should be the preferred reaction path for conversion of **17** to the heart minimum **14** (Figure 5). However, the magnitude of this barrier is high enough to make

(37) Dauben, J. J., Jr.; Wilson, J. D.; Laity, J. L. *Nonbenzenoid Aromatics*; Academic Press: New York, 1971; pp 167−206.
(38) Haberditzl, W. *Angew. Chem., Int. Ed. Engl.* **1966**, *5*, 288−298.
(39) Note that in this system, ring inversion through an open-shell transition state with a planar unit is blocked by benzannulation. See ref 5d and references therein.

Scheme 4. Enthalpy Profiles (CCSD(T)/cc-pVDZ//B3LYP/6-31G* ΔH_0 in kcal/mol) for the Aromatization Pathways of Cyclic Allene **28** and Carbene **29**

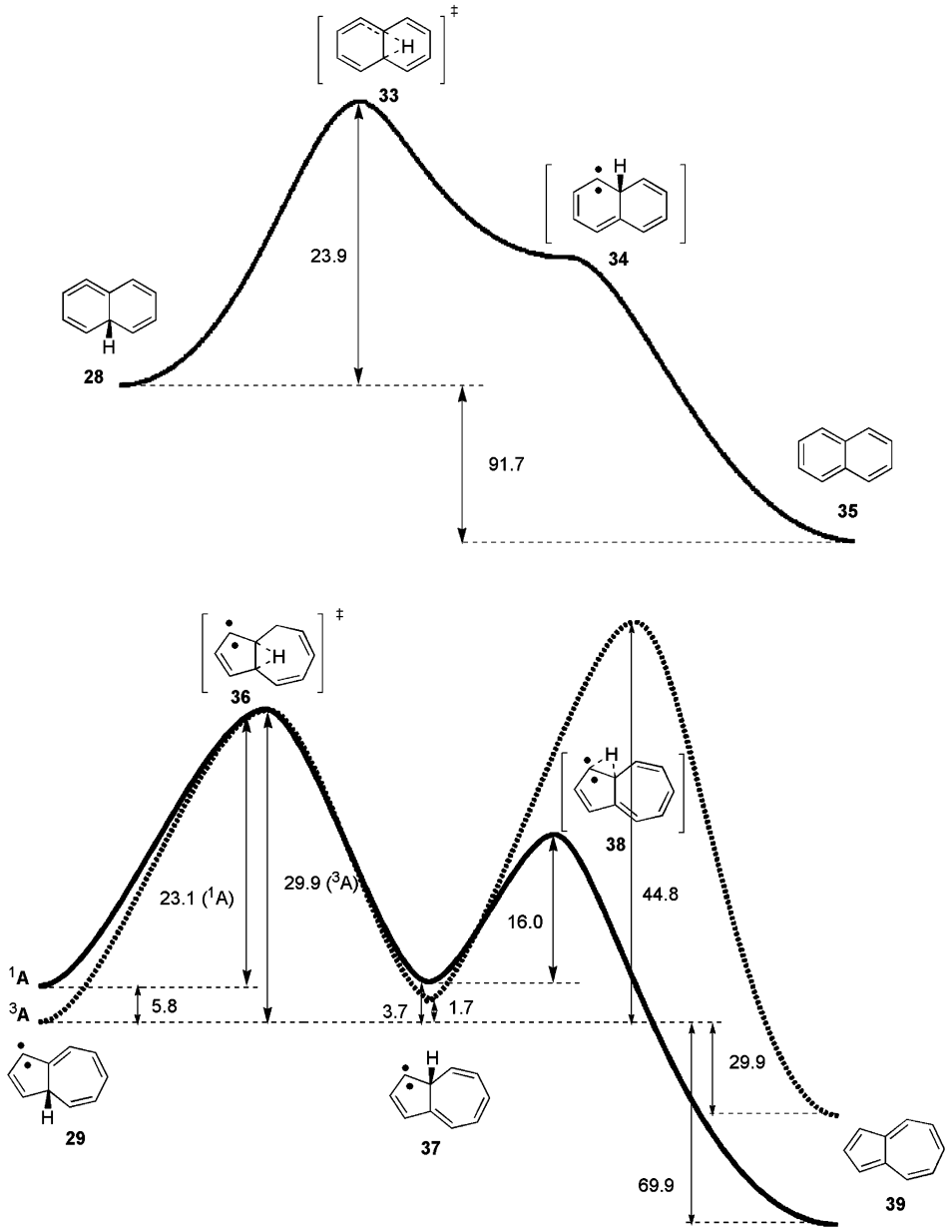

the observation of the twist form **17** in matrix experiments feasible if prepared adequately.

The [5,7]-Cyclizations. Although not yet observed experimentally, the even shorter C^2-C^6 distance relative to the C^1-C^6 distance (2.799 vs 2.844 Å) in the heart form **14** should make a [5,7]-cyclization feasible, leading to the azulene-like carbene **29**. The transition structure **26** associated with this process is positioned later on the PES than transition structure **24**, as judged by the bond distances (Figure 4). Note, however, that the bond indexes for the bonds being formed are very similar, likely due to a large contribution of the π-system in TS **24**. "Late" TS **26** is a consequence of the reaction being significantly more endothermic, $\Delta H_0 = 15.6$ kcal/mol, than the [6,6]-cyclization by nearly 10 kcal/mol at CCSD(T). This difference is due to the much more pronounced biradical character of **29** relative to cyclic allene **28**. In fact, **29** has a triplet ^{3}A ground state 3−6 kcal/mol below the ^{1}A state. Thus, even from the triplet state, the reverse barriers are very low (ca. 7−8 kcal/mol), so this carbene will rearrange very rapidly to the [10]annulene species. The significant activation enthalpy difference favoring the [6,6]-cyclization mode (16.8 vs 23.3 kcal/mol at CCSD(T)) renders [5,7]-fused products unlikely.[40]

However, the [5,7]-cyclization is favored from the twist C_2 form **17**. At CCSD(T) TS, **27** is associated with a 28.2 kcal/mol barrier, which is 2.4 kcal/mol below the [6,6]-cyclization barrier. TS **27** suffers from a minor spin symmetry breaking both at B3LYP/6-31G* and at B3LYP/6-311G** ($\langle S^2\rangle$=0.09 for the latter). Although, as noted above, the reverse barriers for rearrangement of **29** to the heart form **14** are low, it seems to be possible that this intermediate could be intermolecularly trapped by ionic (protic sources) or radical reagents (CCl_4, 1,4-cyclohexadiene)[41] or even bases (Et_3N).[42]

(40) In a recent work studying various phenyl-substituted phenylacetylene substrates, only [6,6]-cyclization products were observed: Rodríguez, D.; Martínez-Esperón, M. F.; Navarro-Vázquez, A.; Castedo, L.; Domínguez, D.; Saá, C. *J. Org. Chem.* **2004**, *69*, 3842−3848.

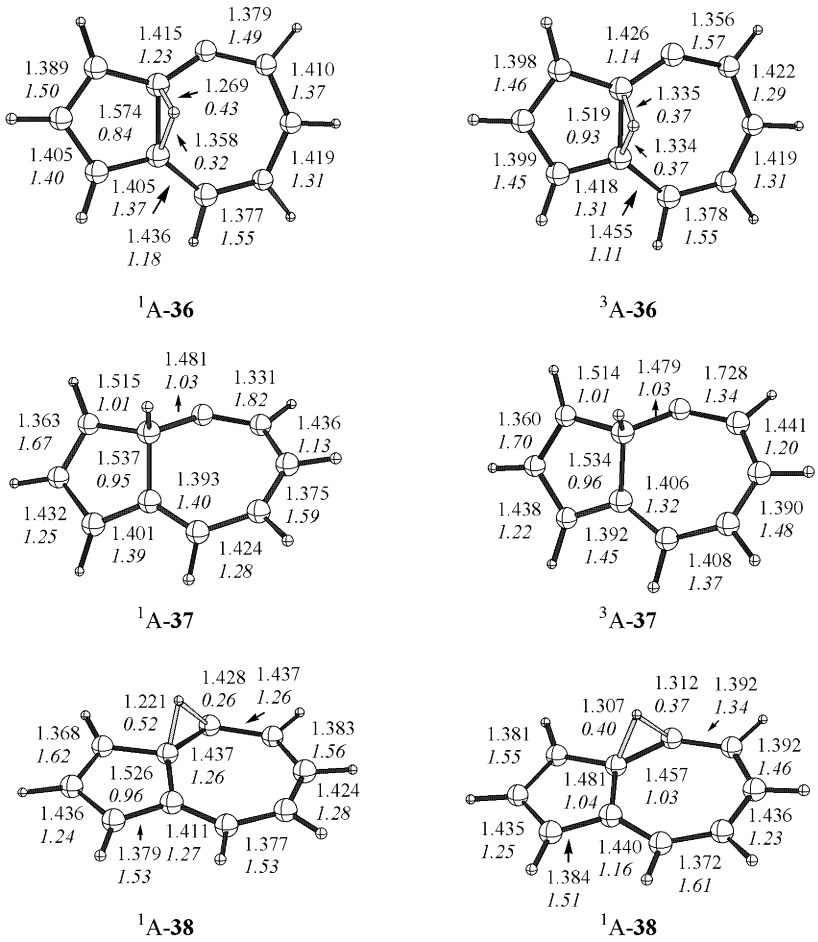

Figure 6. Intermediates and transition structures for aromatization of carbene **28**. Normal bond lengths, italics Wiberg bond indexes on B3LYP/6-311G** densities.

The "Echavarren" Ring-Contraction Mechanism. We also examined the possibility of a ring contraction mechanism as proposed by Echavarren.[2] Contraction of cyclic allene **28** to a tricyclic form **31**, which is placed 28 kcal/mol above the cyclic allene on the singlet surface, takes place through transition structure **30** (Scheme 3) with a very high barrier of 39 kcal/mol (Table 3) that clearly makes this mechanism unlikely compared to the "annulene" mechanism (Scheme 2). We located the very early singlet transition structure **32** (not shown in Scheme 3) that interconnects biradical **31** to the carbene ^{1}A-**29**; after including ZPVE corrections, the barrier vanishes. On the triplet surface, biradical **31** is not a stationary point, and geometry optimization leads to carbene **29**. Note also that for TS **30**, triplet and singlet surfaces are very close in energy, $\Delta H_0 = 0.9$ kcal/mol, favoring the singlet state, and given the structural similarity between triplet and singlet structures, intersystem crossing could take place shortly after passing the transition state in the reaction pathway to ^{3}A-**29**.

3. The Final Step: Aromatization. The aromatization of cyclic allenes has recently been carefully studied both theoretically and experimentally.[5] Deuteration experiments by Saá and co-workers have demonstrated that cyclic allenes can undergo aromatization through reaction with protic donors,[2,43] bases, or halogen atom donors, such as CCl_4.[5d] However, in the absence of such trapping agents, B3LYP and CCSD(T) computations[5d] showed that for isonaphthalene **28** aromatization can also take place through an intramolecular 1,2-shift involving closed-shell transition structure **33** of aromatic character, as evident from NICS computations.[43] Benzannulation causes significant decrease of the barrier; **33** is associated with a 23.9 kcal/mol ΔH_0 barrier at the CCSD(T)/cc-pVDZ//B3LYP/6-31G* level (Table 4), whereas the parent nonbenzannulated cyclohexatriene system isomerizes with a 31.9 kcal/mol barrier at the same level.[5d] Furthermore, for the benzannulated system, the carbene **34** is not a stationary point but an inflection point on the B3LYP/6-31G* surface that directly leads to naphthalene **35** (Scheme 4).

We also investigated a similar aromatization mechanism for the [5,7]-cyclization product **29**. The first step involves a [1,2] hydrogen shift from triplet carbene **29** to the carbene **37** that also has a triplet ground state. The triplet transition structure, ^{3}A-**36**, has a nearly planar geometry and is quite synchronous, as evident from the bond distances (Figure 6). The B3LYP and

(41) This dual polar/radical reactivity is characteristic not only for cyclic allenes but also for molecules with a high biradical character, such as the α,3-didehydrotoluene species: (a) Hughes, T. S.; Carpenter, B. K. *J. Chem. Soc., Perkin Trans. 2* **1999**, 2291−2298. (b) Cremeens, M. E.; Carpenter, B. K. *Org. Lett.* **2004**, *6*, 2349−2352.

(42) Rodríguez, D.; Navarro-Vázquez, A.; Castedo, L.; Domínguez, D.; Saá, C. *Tetrahedron Lett.* **2002**, *43*, 2717−2720.

(43) Rodríguez, D.; Navarro, A.; Castedo, L.; Domínguez, D.; Saá, C. *Org. Lett.* **2000**, *2*, 1497−1500.

Table 5. Relative Energies ΔH_0 (kcal/mol) for Biradical **29** Isomerization

	Species									
level	^{3}A-**29**	^{1}A-**29**	^{3}A-**36**	^{1}A-**36**	^{3}A-**37**	^{1}A-**37**	^{3}A-**38**	^{1}A-**38**	^{3}A-**39**	^{1}A-**39**
B3LYP/6-311G**[a]	0.0	3.6	27.6	27.8	1.5	4.3	38.8	21.0	−33.6	−70.7
MCQDPT2/cc-pVDZ[a]	0.0	−6.8	27.4	22.2	1.2	6.9	39.6	30.7	−14.7	−68.4
UCCSD(T)/cc-pVDZ[a]	0.0	5.8	29.9	28.9	1.7	3.7	44.8	19.7	−29.9	−69.9

[a] Single point on B3LYP/6-31G* geometries.

CCSD(T) levels gave similar activation barriers of 27.6 and 29.9 kcal/mol, respectively (Table 5). When crossing to the singlet surface, this process takes place with barriers of 27.8 and 28.9 kcal/mol at the same levels. The corresponding transition structure, ^{1}A-**36**, is positioned later on the PES than its triplet counterpart. Singlet structure ^{1}A-**29** is preferred in MCQDPT2 computations, which gave a barrier of 29.0 kcal/mol for ^{1}A-**29** → ^{1}A-**37** isomerization. Due to the close structural similarity between the structures on the two surfaces, intersystem crossing is expected to take place easily.

Intermediate carbene **37** isomerizes after intersystem crossing to the ^{1}A state to the final azulene through low-lying closed-shell transition structure ^{1}A-**38**, a structure with closed-shell character, with a barrier of only 16.0 kcal/mol [UCCSD(T)]. Therefore, the first [1,2] H shift is the rate-limiting step. Transition structure ^{3}A-**38** for direct isomerization to triplet $^3B_2$ naphthalene is associated with a much higher barrier (43.1 kcal/mol). Note that for the isomerization to azulene **39** the two electrons provided by the C−H bonds of the migrating hydrogen contribute to a closed-shell aromatic structure in the second transition structure **38** but not in the first step of this isomerization. This is in contrast to the isonaphthalene **28** case, in which this cyclic delocalization can take place already in the first step. Note the better agreement of B3LYP versus MCQDPT2 computations as compared to highest-level coupled-cluster results.

Conclusions

The global conformational minimum of 1,2-didehydro[10]annulenes at the CCSD(T)//B3LYP level is a nearly planar heart aromatic form (**14**) with the (3*Z*,5*E*,7*Z*,9*Z*) configuration. The greater angle strain in the (3*Z*,5*Z*,7*Z*,9*Z*) configuration leads to a localized twist form of Möbius topology (**17**) that is 7 kcal/mol above **14**. Interconversion between these two forms is a slow process and should take place through cyclization to isonaphthalene rather than bond rotation through an antiaromatic Möbius transition structure. Isonaphthalene (cyclic allene) ring-opening to heart 1,2-didehydro[10]annulene has a low barrier (15 kcal/mol), which strongly supports the notion that this structure is a true intermediate in the observed rearrangements in phenylacetylene dehydro Diels−Alder reactions. A ring contraction mechanism seems to be unlikely on the basis of our DFT results. An alternative [5,7]-cyclization mode of annulene **14** to an azulene structure is highly unfavorable both kinetically and enthalpically over the observed [6,6]-cyclization mode, despite the greater proximity of the reaction centers from the heart form. This is, however, the preferred cyclization mode for the C_2 twist form **17** as predicted by CCSD(T) computations.

The aromatization of the [5,7]-cyclization product **29**, a triplet carbene, takes place through two consecutive 1,2 H shifts with a 30 kcal/mol barrier for the first step. The second step, which involves closed-shell "aromatic" 10-electron structure, has a low 16 kcal/mol barrier. In contrast, the aromatization of cyclic allene **28** benefits in the first step from aromatic stabilization.

Acknowledgment. This work was supported by the National Science Foundation (CHE-0209857). A.N. thanks the Spanish Government for granting of a postdoctoral fellowship, and the CESGA for allocation of computer time.

Supporting Information Available: Tables with Cartesian coordinates for all optimized structures, along with tables including absolute energies, ZPVE energies, and $\langle S^2 \rangle$ values; simulated IR spectra and Gaussian archive entries from QCISD computations on species **14** and **17**, and full text for abbreviated references. This material is available free of charge via the Internet at http://pubs.acs.org.

JA0507968